

# *E. coli* DNA replication in the absence of free $\beta$ clamps

Nathan A Tanner<sup>1,2,5</sup>, Gökhan Tolun<sup>3</sup>,  
Joseph J Loparo<sup>1</sup>, Slobodan Jergic<sup>4</sup>,  
Jack D Griffith<sup>3</sup>, Nicholas E Dixon<sup>4</sup>,  
and Antoine M van Oijen<sup>1,2,\*</sup>

<sup>1</sup>Department of Biological Chemistry and Molecular Pharmacology, Harvard Medical School, Boston, MA, USA, <sup>2</sup>Zernike Institute for Advanced Materials, University of Groningen, Groningen, Netherlands, <sup>3</sup>Lineberger Comprehensive Cancer Center, University of North Carolina, Chapel Hill, NC, USA and <sup>4</sup>School of Chemistry, University of Wollongong, Wollongong, New South Wales, Australia

During DNA replication, repetitive synthesis of discrete Okazaki fragments requires mechanisms that guarantee DNA polymerase, clamp, and primase proteins are present for every cycle. In *Escherichia coli*, this process proceeds through transfer of the lagging-strand polymerase from the  $\beta$  sliding clamp left at a completed Okazaki fragment to a clamp assembled on a new RNA primer. These lagging-strand clamps are thought to be bound by the replisome from solution and loaded a new for every fragment. Here, we discuss a surprising, alternative lagging-strand synthesis mechanism: efficient replication in the absence of any clamps other than those assembled with the replisome. Using single-molecule experiments, we show that replication complexes pre-assembled on DNA support synthesis of multiple Okazaki fragments in the absence of excess  $\beta$  clamps. The processivity of these replisomes, but not the number of synthesized Okazaki fragments, is dependent on the frequency of RNA-primer synthesis. These results broaden our understanding of lagging-strand synthesis and emphasize the stability of the replisome to continue synthesis without new clamps.

The EMBO Journal (2011) 30, 1830–1840. doi:10.1038/emboj.2011.84; Published online 25 March 2011

Subject Categories: genome stability & dynamics

Keywords: clamp recycling; DNA replication; fluorescence microscopy; single molecule

## Introduction

The replicative DNA polymerase III of *Escherichia coli* is a heterotrimer of the polymerase subunit  $\alpha$ , the exonuclease  $\epsilon$ , and a stabilizing accessory protein  $\theta$  (McHenry and Crow, 1979; Kelman and O'Donnell, 1995; Johnson and O'Donnell, 2005). This complex, termed the 'core' polymerase, is a relatively distributive enzyme, capable of only

10–20 nucleotide (nt) additions at  $\sim 10 \text{ nt s}^{-1}$  (Fay *et al.*, 1981; Maki *et al.*, 1985). These numbers are dramatically less than is required to replicate the 4.6 mega-basepair (Mb) genome in its 40-min duplication time. To a large extent, polymerase stimulation is conferred by core association with the homodimeric processivity clamp  $\beta$ , which encircles double-stranded DNA (dsDNA) and, through interaction with  $\alpha$ , tethers the polymerase to a primer-template junction (Fay *et al.*, 1981; Georgescu *et al.*, 2008). In complex with  $\beta$ , polymerase activity increases to a rate of 350–500 nt  $\text{s}^{-1}$  and a processivity of 1–2 kilo-basepairs (kb) (Tanner *et al.*, 2008).

The loading of  $\beta$  onto dsDNA is achieved by a multiprotein clamp-loader complex which contains three copies of either a truncated ( $\gamma$ ) or a full-length ( $\tau$ ) version of the *dnaX* gene product, which hydrolyses ATP to open and load  $\beta$  and, with the C-terminal domains of  $\tau$ , binds  $\alpha$  and the helicase DnaB; one copy each of  $\delta$  and  $\delta'$ , which provide structural support for  $\beta$  opening and loading; and the accessory proteins  $\chi$  and  $\psi$ , which interact with single-stranded DNA-binding protein (SSB) and primase DnaG and contribute to regulating the primer handoff cycle (Glover and McHenry, 1998; Jeruzalmi *et al.*, 2001; Johnson and O'Donnell, 2005; Bloom, 2006). The clamp loader and its associated core polymerases form the Pol III\* complex, and addition of the  $\beta$  clamps to Pol III\* forms the holoenzyme (Pol III HE). Since the first analysis of cell lysates, and as depicted in models, the clamp-loader complex has been thought to include one copy of  $\gamma$  and two of  $\tau$ , one each for leading- and lagging-strand polymerases (McHenry and Kornberg, 1977; Onrust *et al.*, 1995). However, recent identification of a  $\tau_3$ -( $\alpha\epsilon\theta$ )<sub>3</sub> replisome and *in vivo* stoichiometry measurements have suggested that the replisome contains three polymerases (McInerney *et al.*, 2007; Reyes-Lamothe *et al.*, 2010). The presence of the additional core has been proposed to have a role in rescuing stalled replisomes or facilitating the lagging-strand cycle for efficient fork progression.

During synthesis of the lagging strand, the active polymerase must cycle from one Okazaki fragment to the next. The polymerase may complete the Okazaki fragment and release upon reaching the 5' end of the previous fragment ('collision' release, Stukenberg *et al.*, 1994; Georgescu *et al.*, 2009), or release before completion of the Okazaki fragment due to a biochemical signal, for example, primer synthesis or other lagging-strand event ('signalling' release, Li and Mariani, 2000; McInerney and O'Donnell, 2004). In either case, the lagging-strand polymerase should disengage from one  $\beta$  clamp and reassociate with another loaded on the new RNA primer. Indeed, biochemical studies demonstrate that a Pol III core quickly releases from  $\beta$  after completing a fragment, and that this core will recycle to a new primed,  $\beta$ -loaded substrate (O'Donnell, 1987; Stukenberg *et al.*, 1994; Georgescu *et al.*, 2009). Traditionally, the  $\beta$  clamp to be loaded on the nascent primer is thought to associate with the replisome from solution. The clamp on the finished fragment is left behind after core dissociation, for binding

\*Corresponding author. Single-Molecule Biophysics, Zernike Institute for Advanced Materials, University of Groningen, Nijenborgh 4, Groningen 9747 AG, Netherlands. Tel.: +31 050 363 9883; Fax: +31 050 363 3660; E-mail: a.m.van.oijen@rug.nl

<sup>5</sup>Present address: New England Biolabs, Ipswich, MA 01938, USA

Received: 27 August 2010; accepted: 28 February 2011; published online: 25 March 2011

other enzymes, such as those involved in Okazaki fragment maturation (Yuzhakov *et al*, 1996; López de Saro and O'Donnell, 2001).

Considering the >10-fold difference between the number of  $\beta$  dimers in the cell ( $\sim 300$ ; Burgers *et al*, 1981) and the number of Okazaki fragments made during chromosome duplication ( $\sim 4000$ ), it is clear that clamps must be reused to allow rapid duplication of the genome. Given that  $\beta$  loaded on circular dsDNA is stable for >60 min without dissociating, the clamps must be actively unloaded (Yao *et al*, 1996). Studies have demonstrated that the forms of the clamp-loader complex and free  $\delta$  are effective clamp unloaders, and this unloading can allow clamps to be reused after subsequent diffusion to the replisome (Naktinis *et al*, 1996; Yao *et al*, 1996; Leu *et al*, 2000). Thus, our current model of the lagging-strand cycle includes a lagging-strand polymerase releasing from a  $\beta$  clamp and associating with a 'new' clamp that has been loaded from solution. However, this mechanism is not completely elucidated; many of the details of clamp unloading and reuse have either not been addressed in the context of coordinated replication by intact replisomes or have been studied using ensemble techniques that can overlook rare or transient events. Here, we use single-molecule fluorescence and electron microscopy to examine replication by complexes unable to complete the traditional lagging-strand clamp-loading cycle.

Our understanding of DNA replication mechanisms is largely based on years of pioneering biochemical experiments that have elucidated the functions and interactions of the various replisome components. Though extremely powerful, traditional ensemble methods inherently obscure rare events, intermediate steps, and even alternate pathways. In recent years, single-molecule methods have been developed to allow the observation of these types of events and have emerged as a powerful complement to traditional bulk-phase techniques, enabling the characterization of primase-induced leading-strand synthesis stalling (Lee *et al*, 2006; Tanner *et al*, 2008), dynamic control of lagging-strand trombone loops (Hamdan *et al*, 2009), priming loops (Manosas *et al*, 2009; Pandey *et al*, 2009) and many other facets of replisome function (reviewed in Hamdan and van Oijen (2010) and van Oijen and Loparo (2010)). We recently demonstrated a technique for visualizing coordinated leading- and lagging-strand synthesis with single-molecule fluorescence microscopy (Tanner *et al*, 2009). By tethering rolling-circle DNA substrates (Mok and Marians, 1987) to the surface of a microscope-mounted flow chamber, we can observe the growing dsDNA product (lagging strand) of a synthesis reaction with a fluorescent DNA stain. This technique has allowed measurement of the rate and processivity of coordinated synthesis by single replisomes (Tanner *et al*, 2009; Yao *et al*, 2009). The real-time visualization of individual replication products allows full characterization of the dynamics of the replication reaction, including the observation of heterogeneity in rates. Furthermore, product lengths of up to hundreds of kb can be measured, far beyond the resolving power of traditional gel electrophoresis measurements.

Here, we adapt the single-molecule rolling-circle assay to facilitate pre-assembly of stable, stalled replisome complexes followed by initiation of synthesis in the absence of free  $\beta$  clamps. Surprisingly, we observed processive synthesis without  $\beta$  in solution, a result that requires either the lagging-

strand polymerase to function without a  $\beta$  clamp or, more consistent with our data, recycling of the  $\beta$  clamp from the end of an Okazaki fragment to a nascent RNA primer. Products synthesized without free clamps were reduced in length and rate as compared with those synthesized under normal conditions, but still contained multiple Okazaki fragments. The absence of free  $\beta$  rendered the processivity of the replisome sensitive to DnaG primase concentration; reducing the concentration of DnaG increased the average product length. We demonstrate that in the absence of free  $\beta$ , the product length increased by the same factor as the spacing of RNA primers, which were still produced and extended in the absence of free  $\beta$ . Together, and in contrast with established dogma, these data demonstrate that the production of multiple Okazaki fragments on the lagging strand can be supported even without the replisome recruiting and loading additional clamps from solution.

## Results

### ***Pre-assembled replisomes produce long replication products***

We have previously shown observation of rolling-circle replication products with single-molecule fluorescence microscopy (Tanner *et al*, 2009). These products are the result of leading-strand synthesis producing a single-stranded 'tail', which is converted to dsDNA by coupling of leading- with lagging-strand synthesis (Figure 1). As the dye (SYTOX Orange) stains only dsDNA, we exclusively observe the products of coupled synthesis. These experiments were performed in the continuous presence of all replisome components, and we observed a product length of  $85.3 \pm 6.1$  kb (fit decay constant  $\pm$  s.e.m.). Yao *et al* (2009) showed that replisomes could be pre-assembled and we adapt their method here. Replisomes were assembled at a primer terminus in a solution containing first DNA, DnaB, and ATP, followed by addition of Pol III HE components and two of the four dNTPs. This solution was diluted and flowed into the chamber, followed by washing with buffer containing the two dNTPs but no replication proteins. Coupled leading- and lagging-strand replication could be observed on introduction of a replication solution containing only DnaG,  $\beta$ , SSB, and all rNTPs and dNTPs. In the pre-assembly reaction, we measured a processivity of  $72.5 \pm 3.5$  kb (Figures 1 and 2). This observation confirms that both Pol III\* and DnaB are efficiently retained at the replication fork (Onrust *et al*, 1995; Yuzhakov *et al*, 1996; Johnson and O'Donnell, 2005; Yao *et al*, 2009). To ensure that the pre-assembly reaction indeed resulted in processive, coordinated leading- and lagging-strand replication by single replisomes, we carried out various control experiments. In particular, omission of only DnaG primase or using exclusively dNTPs in the second-stage replication solution (i.e., with no DnaG,  $\beta$ , or SSB; only pre-assembled Pol III HE components + DnaB) resulted in no detectable products. A reaction with a  $\tau_1\gamma_2\delta\delta'\chi\psi$  (instead of  $\tau_{2/3}\gamma_1\delta\delta'\chi\psi$ ) clamp loader, capable of assembling only one core polymerase in the replisome, yielded no dsDNA products, indicating that a coupled lagging-strand polymerase is required to observe long products. Furthermore, when including SYTOX during the entire reaction including the pre-assembly step, we did not observe product formation until introduction of the replication solution containing all

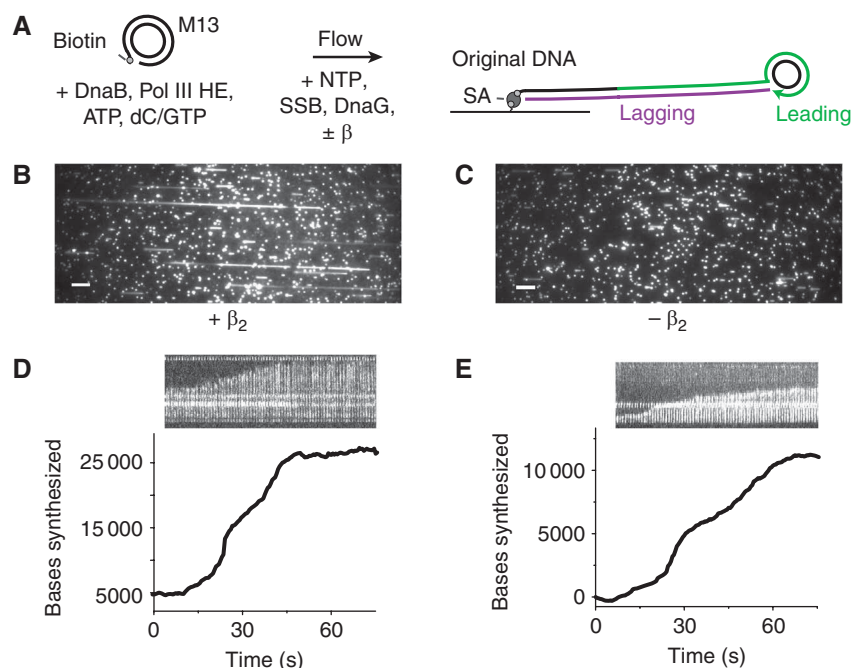


**Figure 1** Visualizing replication products of pre-assembled replisomes. (A) Schematic of pre-assembly reaction. DnaB, Pol III HE components, ATP and two dNTPs are incubated with a pre-filled 5'-biotinylated rolling-circle substrate, which is coupled to a streptavidin-coated coverslip. After removal of free proteins, replication is initiated by addition of all r/dNTPs, SSB, DnaG, and  $\pm \beta$ . (B, C) SYTOX staining of dsDNA *in situ* shows replicated products, with unextended substrates visible as small spots. Regions from fields of view after the full reaction performed with (B) and without (C) free  $\beta$ . Scale bars represent the length of a 10-kb dsDNA product. (D, E) Example molecules from real-time experiments are shown. Kymographs of individual replicating DNA molecules are shown from experiments with (D) and without (E)  $\beta$  in solution. The replication rate can be determined by fitting the end position of the growing molecule with linear regression as described in Tanner *et al* (2009). Shown molecules' average rates are  $661 \text{ bp s}^{-1}$  (D) and  $210 \text{ bp s}^{-1}$  (E); note the different length scales on the ordinates.

NTPs, DnaG, and SSB; during the pre-assembly and wash steps no synthesis was observed. By adding SYTOX only to the replication solution (no stain in pre-assembly or wash mixtures) we can visualize the entrance time of all NTPs, DnaG, etc. into the flow channel, and indeed, product growth occurred directly upon introduction of the SYTOX-containing solution in both  $\beta$ -containing and  $\beta$ -free conditions. These observations clearly establish that the pre-assembled replication complexes were responsible for the observed DNA synthesis.

#### Absence of free $\beta$ does not preclude synthesis

To test whether the  $\beta$  clamps assembled with the replisome were sufficient for coordinated synthesis, we carried out the pre-assembly experiment without any  $\beta$  in the replication reaction, with only the small amount from the Pol III HE component-DnaB pre-assembly mixture. By extensive washing of the flow cell after introduction of the assembled complexes ( $\sim 30$  chamber volumes), we removed any free proteins, leaving only the  $\beta$  that had been loaded onto the leading-strand primer-template and any  $\beta$  associated with the clamp loader or polymerase core. Surprisingly, we observed replication products in the absence of free  $\beta$  which were reduced in length ( $16.6 \pm 1.7 \text{ kb}$  versus  $72.5 \pm 3.5 \text{ kb}$ ; Figures 1C and 2A), but still much longer than a single Okazaki fragment (1–2 kb; Wu *et al*, 1992). Though resulting in processive replication, the efficiency of the reaction was notably decreased in the absence of free  $\beta$  clamps. In the full reaction, we observed 20–50 long products per 100 DNA molecules. With no free  $\beta$  in the reaction, this efficiency

decreased nearly an order of magnitude, to 5–10 products per 100 DNA molecules. The decreased processivity and efficiency of replication may explain why this reaction had not been observed previously, specifically in similar single-molecule experiments limited to observing longer DNA products (Yao *et al*, 2009; Georgescu *et al*, 2010) and ensemble experiments less sensitive to short, inefficient replication (Yuzhakov *et al*, 1996).

#### $\beta$ is efficiently removed from the flow chamber

To demonstrate that no unbound  $\beta$  remained to contribute to synthesis, we extended the washing volume to 250 chamber volumes (using an increased rate of flow, with a wash time of 5–10 min). Not surprisingly, this caused a reduction in the number of products observed ( $< 1$  product per 100 DNA molecules with extended wash versus 5–10 with normal wash) as the pre-assembled complexes are not indefinitely stable and dissociate over time. However, the length of the products was unaffected:  $73.5 \pm 6.6 \text{ kb}$  with  $\beta$  and  $24.5 \pm 3.3 \text{ kb}$  without  $\beta$ . This observation suggests that each replicated molecule is produced using only the  $\beta$  initially loaded with the replisome, without requiring  $\beta$  loading from solution as the fork progresses.

To further confirm that free  $\beta$  molecules were indeed absent from the solution during replication, we repeated the pre-assembly experiment using fluorescently labelled  $\beta$  (Cy5- $\beta$ , see Supplementary data). By imaging the first pre-assembly mixture flowed into the chamber, which contained Cy5- $\beta$  of a known concentration (6 nM after dilution into the flow cell), we can measure the relative background fluores-

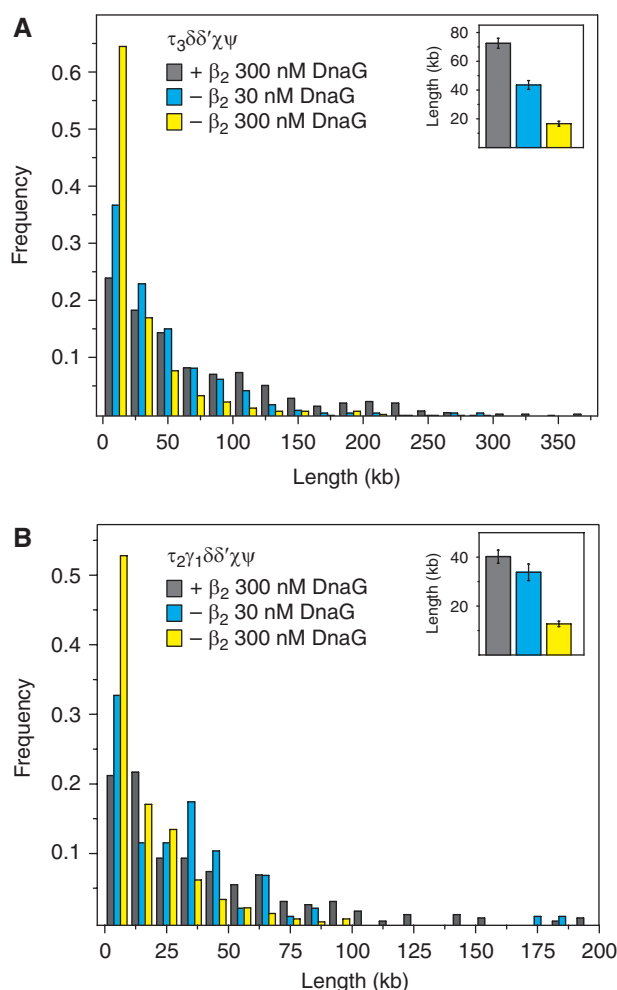


**Figure 2** Product distributions from pre-assembled replisomes. (A) Product lengths from reactions with the  $\tau_3$ -clamp loader. Inset shows values from single-exponential decay constant  $\pm$  s.e.  $N$  indicates the number of molecules observed. Full reaction (+ $\beta_2$ , 300 nM DnaG):  $72.5 \pm 3.5$  kb,  $N = 356$ ; (- $\beta_2$ , 300 nM DnaG):  $16.6 \pm 1.7$  kb,  $N = 366$ ; (- $\beta_2$ , 30 nM DnaG):  $43.5 \pm 3.1$  kb,  $N = 203$ . (B) Products from reactions with the  $\tau_2\gamma_1$ -clamp loader. Full reaction (+ $\beta_2$ , 300 nM DnaG):  $40.2 \pm 2.7$  kb,  $N = 210$ ; (- $\beta_2$ , 300 nM DnaG):  $12.7 \pm 1.1$  kb,  $N = 249$ ; (- $\beta_2$ , 30 nM DnaG):  $33.8 \pm 3.4$  kb,  $N = 85$ .

cence intensity of the solution. The chamber was then washed with buffer, and we imaged again during introduction of the replication solution, which contains no additional  $\beta$ . These images are shown in Supplementary Figure S1, and help establish a minimum concentration reduction due to washing: the measured difference in integrated intensity is 100-fold (59 000 counts during the pre-assembly versus 500 counts during the replication reaction). This reduction results in an upper limit of residual  $\beta$  concentration of  $\sim 60$  pM in our flow cell during the replication reaction. A single-molecule replication experiment with even 200 pM  $\beta$  in the replication solution yielded no products, likely due to the inability to assemble a full Pol III HE. In pre-assembly reactions, the replisome is most efficiently assembled at higher  $\beta$  concentrations. Even assuming that the association time of  $\beta$  with the replisome is diffusion limited, it is clear why such a low concentration would not support replication. Typical experimental conditions use 30–100 nM

$\beta$ , which, using  $1 \times 10^7 \text{ M}^{-1} \text{ s}^{-1}$  as a diffusion-limited bimolecular association rate constant (Creighton, 1993), gives an association time of 1–2 s, on the order of the time required for replisome function. At 60 pM, this association time becomes 1500 s, three orders of magnitude slower than needed for replication. Additionally, the actual concentration of  $\beta$  in solution must be much lower, since much of the measured Cy5- $\beta$  signal can be attributed to  $\beta$  loaded on substrate DNA molecules, as evident in Supplementary Figure S1C. Loaded  $\beta$  is stable on circular DNA for over 60 min, much greater than the timescale of the replication reaction (Yao *et al*, 1996). Thus, the free concentration of  $\beta$  in solution is extremely low, with predicted association times of  $10^4$ – $10^5$  s.

### $\beta$ is loaded only with replisomes

Our reaction was carried out with a mixture of Pol III HE components, which assemble onto DnaB-loaded, primed, and filled M13 DNA substrates (Figure 1A). As  $\beta$  is readily loaded onto primer-template constructs, our results could be explained by multiple  $\beta$  being clamps loaded onto a single DNA substrate during incubation and used over the course of the replication reaction (Bloom *et al*, 1996; Yao *et al*, 1996). To address this possibility, we repeated the pre-assembly reaction using Cy5- $\beta$ . We imaged M13 substrate spots directly after the washing step (using SYTOX and 532 nm laser) and assembled replisomes in the same field (using Cy5- $\beta$  and 640 nm laser). After replication, we identified the M13 molecules that had been replicated, went back in our fluorescence movies to a time point before replication but after assembly, and measured the fluorescence intensity of each corresponding red replisome spot (corresponding to the number of Cy5- $\beta$  molecules). By comparing the intensity trajectory of a replisome spot with the intensity trajectories of single labelled  $\beta$  (measured by flowing 5 pM Cy5- $\beta$  under identical excitation and imaging conditions) we could measure the approximate number of  $\beta$  in the replisome spot. Resulting distributions of intensity decrease and example trajectories are shown in Supplementary Figure S2, and replisome bleaching spots show a 2.5-fold intensity decrease compared with a single labelled  $\beta$ . This is consistent with 2–3 labelled  $\beta$  being assembled with the replisome, not with a DNA coated with additional loaded  $\beta$ . Further demonstrating this stoichiometry, we observed stepwise photobleaching trajectories as shown in Supplementary Figure S2D, a result only possible with a small number of fluorescent dyes. The alternate condition, an M13 substrate completely loaded with protein, was demonstrated with a biotin-primed but unfilled M13 and Cy5-SSB, which will coat the 7.2-kb ssDNA. Imaging the SSB spots under the same conditions resulted in exponential bleaching curves (Supplementary Figure S2E), consistent with many fluorophores in a single spot. Compared with Cy5-SSB alone, which also displayed single photobleaching steps, an SSB-coated ssM13 has  $>30$  Cy5 molecules (saturation reached at  $\sim 65$  Cy5) and resulted in dramatically larger intensity decreases than the  $\beta$  distributions. These data show that our replisome-loaded DNA substrates were not filled with additional  $\beta$  molecules. Our observed low level of  $\beta$  loading could result from not satisfying conditions previously determined for loading of multiple  $\beta$ s, namely the presence of SSB on DNA and both a 5' and 3' primer end (Bloom *et al*, 1996). Also, the first step in our reaction

was loading of DnaB at the fork to facilitate replisome-specific complex assembly, a step that may have prevented extraneous clamp loading.

### Rate of replication decreases in the absence of excess $\beta$ clamps

As described above, both the efficiency and processivity of replication decreased significantly without free  $\beta$  in the replication mixture. With our experimental design, we can also measure rates of replication by single replisomes. By including SYTOX and imaging the replication reaction in real time, we measured the rate of coordinated replication by generating a trajectory of the end point of a growing molecule (Tanner *et al*, 2009). Using the pre-assembly reaction followed by replication in the presence of  $\beta$ , we measured a rate of  $460 \pm 41$  bp s<sup>-1</sup>, similar to the rate of a reaction with all components present (both at 37°C). However, in the absence of free  $\beta$ , the replication rate of a pre-assembled replisome dropped to  $228 \pm 27$  bp s<sup>-1</sup> (examples are shown in Figure 1D and E). A drop in rate would be expected if a lagging-strand core polymerase was extending the RNA primer, though this decrease would be expected to be much greater than the two-fold change we observe (Fay *et al*, 1981). A possible explanation for the two-fold rate decrease would be introduction of a slow intermediate step into the replication mechanism: the need to recycle a  $\beta$  clamp directly from the 3' end of an Okazaki fragment to a nascent primer for the subsequent fragment synthesis. This would effectively introduce a pause in the replication trajectory at the beginning of each new Okazaki fragment, or every 1–2 kb (with 300 nM DnaG). However, the growing DNA end experiences zero stretching force under flow, leading to fluctuations in position that are much beyond the resolution necessary to confidently observe pauses during clamp recycling. Indeed, pauses of duration similar to Okazaki fragment synthesis (2–4 s) would result in an overall halving of the net rate of DNA synthesis.

### Free clamp-absent product length is sensitive to primase concentration

The results described above unexpectedly suggest that the replisome can carry out lagging-strand synthesis without binding and loading a new  $\beta$  clamp. One potential mechanism for overcoming this problem would be the ability to directly reuse a clamp from the end of a completed Okazaki fragment to a new RNA primer. Such a mechanism is expected to have a certain probability of success per Okazaki fragment synthesized. If this idea is correct, the total processivity of the replisome with pre-assembled  $\beta$  should be determined not by the total amount of DNA synthesized, but by the total number of Okazaki fragments produced.

To test this hypothesis, we reduced the concentration of DnaG primase in the reaction from 300 to 30 nM. This reduction has been shown to affect the frequency of DnaG-induced leading-strand synthesis halting (Tanner *et al*, 2008) and increase the length of Okazaki fragments due to similar reduction in priming frequency (Tougu and Mariani, 1996). Here, using a clamp loader with three  $\tau$  domains ( $\tau_3\delta\delta'\chi\psi$ ), we observed that products at low DnaG concentration have a length of  $43.5 \pm 3.1$  kb, which represents a 2.6-fold increase in length compared with the products obtained with

a high DnaG concentration (Figure 2A). Reducing the DnaG concentration had no effect on the replication rate, measured to be  $239 \pm 26$  bp s<sup>-1</sup> with 30 nM DnaG, which is essentially identical to  $228 \pm 27$  bp s<sup>-1</sup> observed with 300 nM DnaG. If the lagging-strand polymerase was synthesizing Okazaki fragments without being bound to a  $\beta$  clamp, it would likely not display sensitivity to primase concentration, as its increased likelihood of dissociation from the primer end affects processivity throughout the synthesis event rather than only upon RNA-primer handoff. This discrepancy suggests the clamp recycling mechanism is the more likely explanation for this observation.

We next sought to test if the replication was facilitated by the presence of the third polymerase in the  $\tau_3$  replisome. Using a clamp loader with two  $\tau$  proteins ( $\tau_2\gamma_1\delta\delta'\chi\psi$ ), with replication observed in the absence of free  $\beta$ , gave products of  $12.7 \pm 1.1$  kb with 300 nM DnaG and  $33.8 \pm 3.4$  kb with 30 nM DnaG (Figure 2B). The measured length increase is a factor of 2.6, identical to the  $\tau_3$  results. However, these lengths are only ~75% of their  $\tau_3$  counterparts, a result that agrees with an overall reduction in synthesis in  $\tau_2$ - versus  $\tau_3$ -mediated replication (McInerney *et al*, 2007). Indeed, when done with  $\beta$  in solution, the  $\tau_2$  reaction gave a processivity of  $40.2 \pm 2.7$  kb, reduced from  $72.5 \pm 3.5$  kb in the  $\tau_3$  reaction. Notably, we observed no products in a reaction with a  $\tau_1\gamma_2\delta\delta'\chi\psi$  clamp loader, verifying that the observed products in other conditions are dependent upon the presence of at least one lagging-strand polymerase and  $\beta$  clamp associated with the pre-assembled replisome. Omitting DnaG from the reaction also produced no products, indicating that priming on the lagging strand is required to produce visible dsDNA products.

### Primase-dependent product length correlates with RNA-primer spacing

The observation that DnaG concentration affects product length in the absence of free  $\beta$  is consistent with the hypothesis that clamps can be recycled according to a fixed recycling probability per Okazaki fragment. Changing the distance between successive RNA primers (clamp loading sites) does not affect the number of cycles but results in an increased overall product length. To further test this interpretation, we analysed the spacing of RNA primers along the length of our DNA products. Reactions were carried out as described above, but in the presence of 150  $\mu$ M digoxigenin-UTP (digUTP) instead of unmodified UTP. Primers synthesized with a U base will thus have a digoxigenin moiety, which can be detected by addition of anti-digoxigenin-functionalized quantum dots (QDs, Figure 3A). Using digUTP in place of UTP does have a slight inhibitory effect on product length: in experiments with free  $\beta$  in solution, the lengths decrease to  $55.7 \pm 3.6$  kb with 300 nM DnaG and  $59.6 \pm 3.1$  kb with 30 nM DnaG. Again, the product length in the presence of excess  $\beta$  was unaffected by a 10-fold reduction in DnaG concentration. The anti-digQDs were added to the flow cell after thorough washing to remove excess digUTP, incubated in the chamber, and washed out with buffer. QDs and SYTOX-stained DNA are imaged with either a 488 or 532 nm laser to preferentially excite the QDs or SYTOX, respectively. Both can be excited at these wavelengths, but the extinction coefficient of the QD at 488 nm (1110 000) is dramatically higher than that of SYTOX (10 000) (Loparo *et al*,



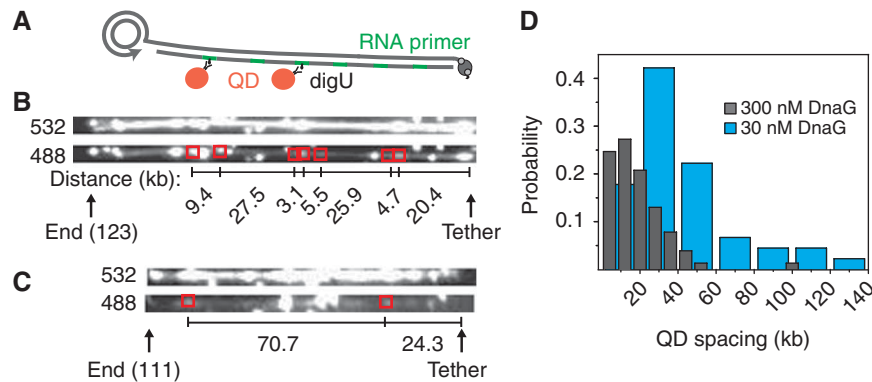


**Figure 3** Visualization of RNA-primer spacing by QD labelling. (A) Experimental design. The pre-assembly reaction is performed with digoxigenin-UTP, which can be detected after incorporation using  $\alpha$ -digQD. (B) Example of DNA replication product after SYTOX staining (300 nM DnaG), imaged with 532 nm (above) or 488 nm (below) laser excitation. DNA-tethered QDs are boxed and spacing between QDs is given in kb. Other non-boxed bright spots are not on the DNA molecule or are bleed-through from SYTOX staining. (C) Example of a DNA replication product obtained with reduced DnaG concentration (30 nM), imaged as in (B). (D) Distribution of QD spacings from 300 and 30 nM DnaG experiments. Distance values are reported as single-exponential fit  $\pm$  s.e.:  $19.8 \pm 2.2$  kb (300 nM DnaG,  $N = 54$ );  $47.3 \pm 6.1$  kb (30 nM,  $N = 44$ ). Fits were performed with the first bin omitted due to undersampling of short spacings.

2011). Switching between the wavelengths allows us to assign signals and eliminate background spots from either stuck QD (a significant amount due to the concentration of digUTP) or uneven SYTOX staining by comparing the relative brightness of a candidate spot at the two wavelengths (Figure 3B). No QDs were observed to bind product DNA when replication reaction did not contain digUTP. QDs on DNA also exhibit Brownian motion from the long DNA fluctuating in flow, and we therefore analysed only QD signals that move with the DNA; surface-immobilized QDs do not move and were not used for analysis (Supplementary Figure S4).

At a high DnaG concentration (300 nM), we observed a QD spacing of  $19.8 \pm 2.2$  kb. This value is obviously much higher than the known Okazaki fragment primer spacing of 1–2 kb (Wu *et al*, 1992; Tougu and Marians, 1996), and the inter-QD distance is larger than the average product length. Thus, our observed QD-DNA molecules represent only the longer dsDNA products. However, we did not expect to tag every RNA primer in the DNA due to inefficient digUTP incorporation by DnaG (incorporation shown in Supplementary Figure S5) and incomplete labelling of DNA-incorporated digUTP with QD (Loparo *et al*, 2011). Nevertheless, we were able to observe long DNA molecules with five or more QD-labelled primers, as shown in Figure 3. In the same experiment, but with a lower DnaG concentration (30 nM), we observed a marked increase in QD spacing, from  $19.8 \pm 2.2$  kb at 300 nM DnaG to  $47.3 \pm 6.1$  kb at 30 nM (Figure 3B–D). Notably, these numbers correspond to a distance increase by a factor of 2.4, nearly identical to the factor of 2.6 observed in product length increase with the same change in DnaG concentration in the absence of free  $\beta$ . This relative increase in distance, rather than the absolute distances, is our measurement of change between the conditions. In the digUTP reaction without free  $\beta$  (300 nM DnaG), we again observed short products ( $15.3 \pm 1.4$  kb) with an identical QD spacing distribution ( $20.5 \pm 3.4$  kb). We observed, in the longer products, multiple QD-labelled primers in single DNA molecules, verifying that in the absence of free  $\beta$ , multiple priming cycles take place on the lagging strand.

### Okazaki fragment spacing observed with electron microscopy

Even though the above data demonstrate multiple productive lagging-strand priming events by single replisomes, the QD-labelled RNA primers represent only a small fraction of the actual RNA primers along the DNA. To further substantiate our observations, we analysed rolling-circle DNA products using electron microscopy. Replication reactions were carried out using protein concentrations as described above and products were cross-linked with glutaraldehyde, purified by size-exclusion column chromatography, and then mounted on EM grids (see Materials and Methods). We observed long product tails extending from the DNA substrate (Figure 4). As noted with arrows, we observed changes in density periodically along the tail, regions that resemble SSB-coated ssDNA.

In typical depictions of DNA replication, Okazaki fragments are filled in completely to the 5' end of the previous fragment. As described above, however, two competing models control release and recycling of the lagging-strand polymerase: in the signalling model, synthesis of a nascent RNA primer signals release of the lagging-strand polymerase; in the collision model, the lagging-strand polymerase collides with the 5' end of the previous fragment and releases to a new primer. Data exist to support both models (O'Donnell, 1987; Stukenberg *et al*, 1994; Yuzhakov *et al*, 1996; Li and Marians, 2000; McInerney and O'Donnell, 2004; Georgescu *et al*, 2009), and single-molecule analysis of replication loops in the phage T7 system suggests an equal prevalence of these mechanisms (Hamdan *et al*, 2009). In our EM images, collision model Okazaki fragments cannot be seen without enzymatic treatment of the products (Chastain *et al*, 2000), but any signalling fragments will have a ssDNA gap between the 3' end of an Okazaki fragment and the 5' end of the previous fragment. In this experiment, we 'stain' the product DNA with additional SSB, giving rise to regions of high density along the DNA. With an approximately equal contribution by collision- and signalling-mediated fragments, we expect to see only half of the Okazaki fragment junctions as revealed by SSB-coated ssDNA gaps left by the signalling mechanism.

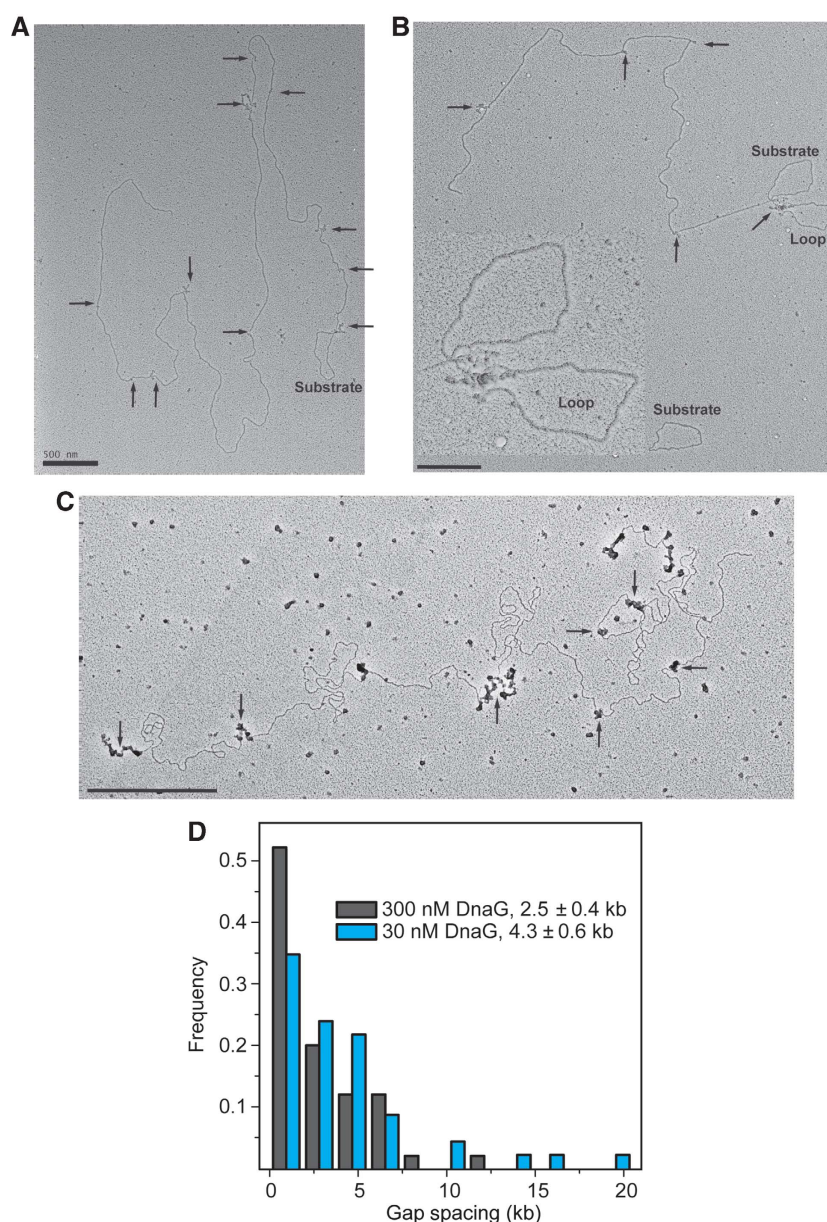


**Figure 4** Electron microscopy of replication products. (A) Example of DNA replication product (300 nM DnaG) is shown. Arrows indicate ssDNA gaps along the lagging-strand tail. (B) Example of DNA replication product at reduced DnaG concentration (30 nM) is shown. Inset shows a blow-up of the replication loop visible at the fork. (A, B) are mounted with cytochrome *c* drop spreading. (C) Direct mounted sample with ssDNA clearly seen through SSB staining. (D) Gap-spacing distribution. Numbers represent single-exponential fit  $\pm$  s.e.m. (300 nM DnaG:  $N = 50$ ; 30 nM DnaG:  $N = 46$ ).

Indeed, our observed spacing at 300 nM DnaG is  $2.5 \pm 0.4$  kb, approximately twice the average Okazaki fragment length at that primase concentration ( $\sim 1$ – $2$  kb; Tougu and Mariani, 1996). Decreasing the DnaG concentration to 30 nM as in previously described experiments resulted in a gap spacing of  $4.3 \pm 0.6$  kb, an increase of 1.7-fold (Figure 4D). This increase is consistent with the increased QD distances described above. Also confirming that observed replication products were indeed a result of coordinated leading- and lagging-strand synthesis from single replisomes, we were able to observe trombone loops on some of the cross-linked EM samples (Figure 4B; Chastain *et al*, 2003). Reactions carried out in the absence of  $\beta$  were done in our fluorescence

microscope flow cells using fluorescent SSB, allowing visualization of ssDNA spacing without  $\beta$ . We observed similar patterns of multiple SSB spots along the DNA product, further indicating that without free  $\beta$  we indeed produce multiple rounds of Okazaki fragment synthesis (Supplementary Figure S6). We used electron microscopy for spacing data shown above to achieve higher resolution and to enable observation of replication loops. In summary, we demonstrate that our observed effect of DnaG concentration on product length in the absence of free  $\beta$  corresponds directly with changes in RNA-primer spacing, supporting the hypothesis that replisome-associated  $\beta$  clamps can be recycled on the lagging strand.

## Discussion

In *E. coli*, lagging-strand synthesis is a dynamic process, requiring synthesis of an RNA primer, loading of a  $\beta$  clamp on the primer, association of a lagging-strand polymerase with the loaded  $\beta$ , and extension of the RNA primer to form an Okazaki fragment. This cycle repeats  $\sim 2000$  times per replication fork, and is mediated by multiple protein-protein interactions among  $\chi\psi$ , DnaG, DnaB, SSB,  $\tau$ ,  $\beta$ , and  $\alpha\epsilon\theta$ . Biochemical data support the generally accepted model in which a new  $\beta$  clamp is loaded on each primer and the lagging-strand polymerase releases from its current  $\beta$  to associate with the new one for extension of the primer (O'Donnell, 1987; Stukenberg *et al*, 1994; Yuzhakov *et al*, 1996; Li and Mariani, 2000; Georgescu *et al*, 2009). However, considering the low concentration of  $\beta$  in the cell ( $\sim 300$   $\beta$  dimers; Burgers *et al*, 1981) and the need for loading  $1\text{--}2$   $\beta\text{ s}^{-1}$  for 40 min, some mechanism must exist for recycling  $\beta$  clamps: each clamp must be used roughly 10 times to completely duplicate the genome. Free  $\delta$  subunit and clamp-loading complexes can also unload  $\beta$  from DNA into solution, presumably to then be reused by the replisome (Naktinis *et al*, 1996; Yao *et al*, 1996; Leu *et al*, 2000). Data measuring the accumulation of  $\beta$  along lagging-strand products from pre-assembled replisomes measured only 33% of the expected amount of one  $\beta_2$  per Okazaki fragment, suggesting that the replisome indeed unloads  $\beta$  as it proceeds during synthesis (Yuzhakov *et al*, 1996). Clamp unloading by the  $\gamma_3$  clamp-loader complex alone is not significantly faster than an intact Pol III\* (Leu *et al*, 2000), thus a full replisome can unload clamps efficiently. Similarly, the replisome may not always have a  $\beta$  ready to be loaded for each primer. The data presented here suggest that the replisome can continue synthesis of the lagging strand even in cases when a new clamp cannot be loaded from solution.

We observed processive, coupled leading- and lagging-strand synthesis by pre-assembled replisomes in the absence of any  $\beta$  in solution. Any  $\beta$  clamps used in the reaction were from  $\beta$  loaded with the replisome in our pre-assembly reaction, which assembles single replisome complexes on rolling-circle substrates and facilitates removal of all free proteins before initiation of synthesis (Yao *et al*, 2009). Interestingly, we observed that the product length in the absence of free  $\beta$  can be modulated by changing the concentration of DnaG primase. Reactions with  $\beta$  in the replication mixture do not display differential product lengths at equivalent DnaG concentrations, suggesting that products made without free  $\beta$  resulted from lower-probability replisome-mediated recycling of the  $\beta$  clamp to a new primer. This primase concentration-modulated length change scaled identically to changes in RNA-primer spacing and Okazaki fragment spacing distributions, as shown with single-molecule fluorescence and EM data. Together, these data support a mechanism by which a  $\beta$  clamp can be recycled for  $\sim 10$  lagging-strand cycles, from a completed or signal-terminated Okazaki fragment to a nascent RNA primer.

This clamp recycling implies that at least two  $\beta$  clamps were pre-assembled with the replisome: one loaded on the leading-strand primer-template and another bound to the clamp-loader complex or perhaps to a lagging-strand polymerase. Our measurements of 2–3  $\beta$  assembled with the replisome support this requirement, and the clamp loader

in the replisome must by definition be capable of binding additional clamps during synthesis. It is reasonable to conclude that the pre-assembled complex may contain  $>1$   $\beta$  clamp, one loaded onto a primer-template junction and another awaiting a 3' end for loading (Park and O'Donnell, 2009). The need for dynamic clamp association is inherent to replisome progression, and stoichiometry measurements from living cells detect 2–3 clamps in the replisome as expected (Reyes-Lamothe *et al*, 2010). In our experiments, no dsDNA synthesis was observed without DnaG or with a leading strand only replisome ( $\tau_1\gamma_2\delta\delta'\chi\psi:(\alpha\epsilon\theta)_1$ ), and we observed numerous RNA primers and ssDNA gaps along the product DNA, indicating that the replication we observe is the result of true lagging-strand Okazaki fragment synthesis. Our data showed more efficient synthesis using a three-polymerase replisome, in agreement with previous reports (McInerney *et al*, 2007), likely due to stimulation of overall replication ability in the presence of an additional polymerase. The  $\tau_3:(\alpha\epsilon\theta)_3$  replisome may simply be more stable as an assembled complex, giving rise to more and longer products in our experiments, as well as the greater synthesis observed previously (McInerney *et al*, 2007). The extra  $\tau$  domain may help protect the lagging-strand  $\beta$  from dissociation similar to its protection on the leading strand (Kim *et al*, 1996). In our experiments, we assemble replisomes with a mixture of Pol III HE components and wash out free protein, and as described above the remaining trace amounts are extremely low. Thus, we cannot completely exclude the possibility of unloading effects from free clamp-loader complexes, though due to concentration and association times this is extremely unlikely.

An alternate explanation for our data is synthesis of Okazaki fragments by a lagging-strand core polymerase without a  $\beta$  clamp. This mechanism is unlikely, as the rate of synthesis and processivity of Pol III alone are much too low for synthesis of a 1–2 kb Okazaki fragment in 2–4 s, even in the presence of  $\tau$  and SSB-coated ssDNA (Fay *et al*, 1981). Our observed two-fold decrease in rate and multiple Okazaki fragments in reactions without free  $\beta$  are inconsistent with expectations of lagging-strand synthesis by core polymerases alone, though the efficiency of  $\beta$ -free lagging-strand polymerase tethered to a progressing replisome that includes a leading-strand  $\beta$  is unknown (and would be exceedingly difficult to determine). On the other hand, there is strong evidence that  $\beta$  is required for efficient lagging-strand synthesis. Experiments using pre-assembled replication complexes report a requirement for additional  $\beta$  to enable lagging-strand synthesis both in bulk experiments with isolated complexes (Yuzhakov *et al*, 1996) and in single-molecule assays using a set-up similar to ours (Yao *et al*, 2009). These methods were capable of detecting only either efficient DNA synthesis (Yuzhakov *et al*, 1996) or synthesis of long ( $>30$  kb) products (Yao *et al*, 2009). In contrast, we are able to detect short and rare lagging-strand replication events that appear to rely on the presence of a second  $\beta$  molecule bound in the replisome. Furthermore, the dependence of product length on DnaG concentration when clamps are absent is inconsistent with the lagging-strand polymerase catalysing synthesis without a  $\beta$  clamp.

We propose that the likely explanation for our data is direct replisome-mediated recycling of a  $\beta$  clamp from a finished Okazaki fragment to the start of a new fragment.



This mechanism could serve to ensure fork progression without stalling when a new  $\beta$  clamp is not readily available from solution. Inherent to this model is the requirement of the clamp-loader complex at the fork to unload a  $\beta$  clamp from the product dsDNA and re-load it on the nascent primer, with an active competition between recycling of the old clamp and the preferred mechanism, loading one recruited from solution. If an additional clamp binds the replisome during Okazaki fragment synthesis, the used clamp is left behind and the lagging-strand polymerase core is transferred to a new primer terminus. When an additional clamp is not bound, the used clamp and polymerase can be transferred together and a  $\beta$  clamp is not left behind at the end of the Okazaki fragment.

Recent work has suggested an increasingly dynamic picture of the replisome (Langston *et al.*, 2009), with components exchanging during replication (Hamdan *et al.*, 2007) and different mechanisms controlling replication loop formation and release (Hamdan *et al.*, 2009). In *E. coli*, three each of core polymerase,  $\tau$ , and  $\beta_2$  are now thought to be in the replisome (McInerney *et al.*, 2007; Reyes-Lamothé *et al.*, 2010) and accessory proteins associate directly with the replisome during replication (Heltzel *et al.*, 2009; Indiani *et al.*, 2009; Langston *et al.*, 2009). The reuse of  $\beta$  clamps may also be more complicated, with potential recycling and effects of other protein interactions (López de Saro and O'Donnell, 2001). Further study of clamp dynamics in active replisomes will allow a greater understanding of how replication proteins are used and recycled during lagging-strand synthesis. Previous work has shown the ability of the replisome to overcome blockage from DNA damage (Indiani *et al.*, 2009) and RNA polymerase complexes (Pomerantz and O'Donnell, 2010). Continuation of synthesis without binding and loading of a new  $\beta$  clamp similarly demonstrates the stability and flexibility of the replisome and the variety of mechanisms that ensure complete genome duplication.

## Materials and methods

### Pre-assembly reaction

Replication proteins were prepared as described (Tanner *et al.*, 2008, 2009). Conditions for pre-assembly of an initiation complex were adapted from Yao *et al.* (2009). Briefly, 60 nM DnaB<sub>6</sub> was incubated with 1.5 nM biotinylated-M13 substrate in replication buffer (50 mM HEPES pH 7.9, 80 mM KCl, 12 mM Mg(OAc)<sub>2</sub>, 0.1 mg ml<sup>-1</sup> BSA, and 5 mM dithiothreitol) with 1.25 mM ATP at 37°C for 30 s (solution 1). Pol III HE components were added as 27 nM  $\tau_3\delta\delta'\chi\psi$  (or other clamp-loader complex where indicated), 74 nM  $\beta_2$ , 81 nM  $\alpha\epsilon\theta$  in replication buffer with 60  $\mu$ M dCTP and dGTP (New England Biolabs) only (solution 2). Next, 20  $\mu$ l of (solution 2) was added to 20  $\mu$ l of (solution 1) and incubated at 37°C for 6 min. This mixture was diluted with 200  $\mu$ l of replication buffer with 60  $\mu$ M dCTP and dGTP (wash buffer) and flowed over the streptavidin-coated surface of the flow chamber (see below, Tanner and van Oijen, 2010) at 0.120 ml min<sup>-1</sup> for 1 min followed by 0.02 ml min<sup>-1</sup> for 1 min. To remove free proteins, the flow cell was then washed with 100  $\mu$ l of wash buffer (~30 chamber volumes over 2–3 min). DNA synthesis was initiated by flowing solution 3: replication buffer with 1 mM ATP, 250  $\mu$ M CTP, GTP, and UTP (GE Life Sciences), 60  $\mu$ M dCTP, dGTP, dATP, and dTTP, 300 nM or 30 nM DnaG, 450 nM SSB<sub>4</sub>, and 50 nM  $\beta_2$  where indicated.

### Fluorescence imaging of DNA replication

The flow chamber and PEG-biotin-functionalized surfaces were prepared as described in Tanner and van Oijen (2010). The flow

chamber was constructed using a streptavidin-coated PEG-biotin glass coverslip, a 1.5 mm channel cut from double-sided tape (Grace Biolabs), and a quartz slide (Technical Glass) with holes drilled for attachment of polyethylene tubing (Becton Dickinson, 0.76 mm inner diameter). The chamber was blocked with buffer containing 0.2 mg ml<sup>-1</sup> BSA and 0.005% Tween-20 to minimize non-specific interactions with proteins, DNA, and QDs. The chamber was placed on an inverted microscope (Olympus IX-71) with  $\times 60$  oil-immersion TIRF objective (NA 1.45, Olympus) and connected to a syringe pump (Harvard Apparatus) for flow of buffer. DNA was stained with 25 nM SYTOX Orange (Invitrogen) excited by a 532-nm laser (Coherent, Compass 215M-75) and imaged on an EMCCD camera (Hamamatsu, ImageEM). Reactions were at 37°C, maintained by attaching a home-built aluminium block to the top of the quartz slide, heated by a cartridge heater controlled by a variable power supply (Tanner and van Oijen, 2010). Fluorescent proteins were labelled with homemade NHS-ester-Cy3-Cy5 (see Supplementary data) and excited with 641 nm laser (Coherent, Cube 641–100 mW); 488, 532, and 641 nm beams were overlapped using dichroic mirrors and fluorescence filtered with appropriate filter sets (Chroma).

### RNA-primer visualization

To measure spacings between RNA primers, the pre-assembly reaction was as described above, but with solution 3 containing CTP and GTP at 150, and 150  $\mu$ M UTP-11-digoxigenin (digUTP, Roche) in place of UTP. After synthesis, the flow chamber was washed extensively with replication buffer to remove free digUTP. QDs (Invitrogen QDot 605) were functionalized with sheep  $\alpha$ -digoxigenin Fab (Roche) using the manufacturer's protocol (Invitrogen QDot Antibody Coupling Kit). QD was imaged with a 488-nm laser (Coherent, Sapphire 488-50), which excites them favourably over SYTOX Orange. Conversely, imaging SYTOX with a 532-nm laser biases the excitation towards SYTOX. By taking images with 488 and 532 nm excitation, we were able to observe single DNA molecules and any QD-tagged primers while controlling for any aberrant DNA staining (SYTOX-bright spots) and non-specifically surface-adhered QD (no Brownian fluctuation as with DNA-tethered QD; Supplementary Figure S4).

### Electron microscopy of replication products

Replication reactions were carried out in bulk using concentrations of components as above, but with a smaller substrate (3 kb pGLGAP plasmid DNA with ~500 nt long displaced ssDNA tail; Subramanian and Griffith, 2005) and incubated for 90 s at 37°C. Reaction products were then either fixed by immediate addition of 0.6% v/v glutaraldehyde and/or quenched with 100 mM EDTA. Products were purified by passing them through 6% plain agarose bead (Agarose Bead Technologies) columns. Samples not fixed with glutaraldehyde were treated with 0.5  $\mu$ g ml<sup>-1</sup> SSB and then fixed to mark any ssDNA. Samples were then mounted onto grids by following either direct mounting or cytochrome c drop-spreading methods as described (Griffith and Christiansen, 1978; Lee *et al.*, 2002). The samples were then examined in an FEI Tecnai 12 TEM and the images recorded using an Ultrascan400 CCD camera (Gatan Inc.).

### Supplementary data

Supplementary data are available at *The EMBO Journal* Online (<http://www.embojournal.org>).

## Acknowledgements

NAT, GT, JLL, and AMvO designed experiments. NAT and JLL performed single-molecule experiments. NAT, GT, and JDG performed electron microscopy. NAT and GT analysed single-molecule and electron microscopy data, respectively. SJ purified replication proteins. NAT, JLL, SJ, NED, and AMvO conceived the study and wrote the manuscript. Work was supported by the National Institutes of Health (AMvO) and the Australian Research Council (NED).

## Conflict of interest

The authors declare that they have no conflict of interest.

## References

- Bloom LB (2006) Dynamics of loading the *Escherichia coli* DNA polymerase processivity clamp. *Crit Rev Biochem Mol Biol* **41**: 179–208
- Bloom LB, Turner J, Kelman Z, Beechem JM, O'Donnell M, Goodman MF (1996) Dynamics of loading the  $\beta$  sliding clamp of DNA polymerase III onto DNA. *J Biol Chem* **271**: 30699–30708
- Burgers PM, Kornberg A, Sakakibara Y (1981) The *dnaN* gene codes for the  $\beta$  subunit of DNA polymerase III holoenzyme of *Escherichia coli*. *Proc Natl Acad Sci USA* **78**: 5391–5395
- Chastain II PD, Makhov AM, Nossal NG, Griffith JD (2000) Analysis of the Okazaki fragment distributions along single long DNAs replicated by the bacteriophage T4 proteins. *Mol Cell* **6**: 803–814
- Chastain II PD, Makhov AM, Nossal NG, Griffith JD (2003) Architecture of the replication complex and DNA loops at the fork generated by the bacteriophage T4 proteins. *J Biol Chem* **278**: 21276–21285
- Creighton TE (1993) *Proteins: Structures and Molecular Properties*, 2nd edn, New York: W.H. Freeman
- Fay PJ, Johanson KO, McHenry CS, Bambara RA (1981) Size classes of products synthesized processively by DNA polymerase III and DNA polymerase III holoenzyme of *Escherichia coli*. *J Biol Chem* **256**: 976–983
- Georgescu RE, Kim SS, Yurieva O, Kuriyan J, Kong XP, O'Donnell M (2008) Structure of a sliding clamp on DNA. *Cell* **132**: 43–54
- Georgescu RE, Kurth I, Yao NY, Stewart J, Yurieva O, O'Donnell M (2009) Mechanism of polymerase collision release from sliding clamps on the lagging strand. *EMBO J* **28**: 2981–2991
- Georgescu RE, Yao NY, O'Donnell M (2010) Single-molecule analysis of the *Escherichia coli* replisome and use of clamps to bypass replication barriers. *FEBS Lett* **584**: 2596–2605
- Glover BP, McHenry CS (1998) The  $\chi\psi$  subunits of DNA polymerase III holoenzyme bind to single-stranded DNA-binding protein (SSB) and facilitate replication of an SSB-coated template. *J Biol Chem* **273**: 23476–23484
- Griffith JD, Christiansen G (1978) Electron microscope visualization of chromatin and other DNA-protein complexes. *Annu Rev Biophys Bioeng* **7**: 19–35
- Hamdan SM, Johnson DE, Tanner NA, Lee JB, Qimron U, Tabor S, van Oijen AM, Richardson CC (2007) Dynamic DNA helicase-DNA polymerase interactions assure processive replication fork movement. *Mol Cell* **27**: 539–549
- Hamdan SM, Loparo JJ, Takahashi M, Richardson CC, van Oijen AM (2009) Dynamics of DNA replication loops reveal temporal control of lagging-strand synthesis. *Nature* **457**: 336–339
- Hamdan SM, van Oijen AM (2010) Timing, coordination, and rhythm: acrobatics at the DNA replication fork. *J Biol Chem* **285**: 18979–18983
- Heltzel JM, Maul RW, Scouten Ponticelli SK, Sutton MD (2009) A model for DNA polymerase switching involving a single cleft and the rim of the sliding clamp. *Proc Natl Acad Sci USA* **106**: 12664–12669
- Indiani C, Langston LD, Yurieva O, Goodman MF, O'Donnell M (2009) Translesion DNA polymerases remodel the replisome and alter the speed of the replicative helicase. *Proc Natl Acad Sci USA* **106**: 6031–6038
- Jeruzalmi D, O'Donnell M, Kuriyan J (2001) Crystal structure of the processivity clamp loader gamma ( $\gamma$ ) complex of *E. coli* DNA polymerase III. *Cell* **106**: 429–441
- Johnson A, O'Donnell M (2005) Cellular DNA replicases: components and dynamics at the replication fork. *Annu Rev Biochem* **74**: 283–315
- Kelman Z, O'Donnell M (1995) DNA polymerase III holoenzyme: structure and function of a chromosomal replicating machine. *Annu Rev Biochem* **64**: 171–200
- Kim S, Dallmann HG, McHenry CS, Mariani KJ (1996)  $\tau$  protects  $\beta$  in the leading-strand polymerase complex at the replication fork. *J Biol Chem* **271**: 4315–4318
- Langston LD, Indiani C, O'Donnell M (2009) Whither the replisome: emerging perspectives on the dynamic nature of the DNA replication machinery. *Cell Cycle* **8**: 2686–2691
- Lee J, Chastain II PD, Griffith JD, Richardson CC (2002) Lagging strand synthesis in coordinated DNA synthesis by bacteriophage T7 replication proteins. *J Mol Biol* **316**: 19–34
- Lee JB, Hite RK, Hamdan SM, Xie XS, Richardson CC, van Oijen AM (2006) DNA primase acts as a molecular brake in DNA replication. *Nature* **439**: 621–624
- Leu FP, Hingorani MM, Turner J, O'Donnell M (2000) The  $\delta$  subunit of DNA polymerase III holoenzyme serves as a sliding clamp unloader in *Escherichia coli*. *J Biol Chem* **275**: 34609–34618
- Li X, Mariani KJ (2000) Two distinct triggers for cycling of the lagging strand polymerase at the replication fork. *J Biol Chem* **275**: 34757–34765
- Loparo JJ, Kulczyk AW, Richardson CC, van Oijen AM (2011) Simultaneous single-molecule measurements of bacteriophage T7 replisome composition and function reveal the mechanism of polymerase exchange. *Proc Natl Acad Sci USA* **108**: 3584–3589
- López de Saro FJ, O'Donnell M (2001) Interaction of the  $\beta$  sliding clamp with MutS, ligase, and DNA polymerase I. *Proc Natl Acad Sci USA* **98**: 8376–8380
- Maki H, Horiuchi T, Kornberg A (1985) The polymerase subunit of DNA polymerase III of *Escherichia coli*. I. Amplification of the *dnaE* gene product and polymerase activity of the  $\alpha$  subunit. *J Biol Chem* **260**: 12982–12986
- Manosas M, Spiering MM, Zhuang Z, Benkovic SJ, Croquette V (2009) Coupling DNA unwinding activity with primer synthesis in the bacteriophage T4 primosome. *Nat Chem Biol* **5**: 904–912
- McHenry C, Kornberg A (1977) DNA polymerase III holoenzyme of *Escherichia coli*. Purification and resolution into subunits. *J Biol Chem* **252**: 6478–6484
- McHenry CS, Crow W (1979) DNA polymerase III of *Escherichia coli*. Purification and identification of subunits. *J Biol Chem* **254**: 1748–1753
- McInerney P, Johnson A, Katz F, O'Donnell M (2007) Characterization of a triple DNA polymerase replisome. *Mol Cell* **27**: 527–538
- McInerney P, O'Donnell M (2004) Functional uncoupling of twin polymerases: mechanism of polymerase dissociation from a lagging-strand block. *J Biol Chem* **279**: 21543–21551
- Mok M, Mariani KJ (1987) Formation of rolling-circle molecules during  $\phi$ X174 complementary strand DNA replication. *J Biol Chem* **262**: 2304–2309
- Naktinis V, Turner J, O'Donnell M (1996) A molecular switch in a replication machine defined by an internal competition for protein rings. *Cell* **84**: 137–145
- O'Donnell ME (1987) Accessory proteins bind a primed template and mediate rapid cycling of DNA polymerase III holoenzyme from *Escherichia coli*. *J Biol Chem* **262**: 16558–16565
- Onrust R, Finkelstein J, Naktinis V, Turner J, Fang L, O'Donnell M (1995) Assembly of a chromosomal replication machine: two DNA polymerases, a clamp loader, and sliding clamps in one holoenzyme particle. I. Organization of the clamp loader. *J Biol Chem* **270**: 13348–13357
- Pandey M, Syed S, Donmez I, Patel G, Ha T, Patel SS (2009) Coordinating DNA replication by means of priming loop and differential synthesis rate. *Nature* **462**: 940–943
- Park MS, O'Donnell M (2009) The clamp loader assembles the  $\beta$  clamp onto either a 3' or 5' primer terminus: the underlying basis favoring 3' loading. *J Biol Chem* **284**: 31473–31483
- Pomerantz RT, O'Donnell M (2010) Direct restart of a replication fork stalled by a head-on RNA polymerase. *Science* **327**: 590–592
- Reyes-Lamothe R, Sherratt DJ, Leake MC (2010) Stoichiometry and architecture of active DNA replication machinery in *Escherichia coli*. *Science* **328**: 498–501
- Stukenberg PT, Turner J, O'Donnell M (1994) An explanation for lagging strand replication: polymerase hopping among DNA sliding clamps. *Cell* **78**: 877–887
- Subramanian D, Griffith JD (2005) p53 monitors replication fork regression by binding to 'chickenfoot' intermediates. *J Biol Chem* **280**: 42568–42572
- Tanner NA, Hamdan SM, Jergic S, Loscha KV, Schaeffer PM, Dixon NE, van Oijen AM (2008) Single-molecule studies of fork dynamics in *Escherichia coli* DNA replication. *Nat Struct Mol Biol* **15**: 170–176
- Tanner NA, Loparo JJ, Hamdan SM, Jergic S, Dixon NE, van Oijen AM (2009) Real-time single-molecule observation of rolling-circle DNA replication. *Nucleic Acids Res* **37**: e27
- Tanner NA, van Oijen AM (2010) Visualizing DNA replication at the single-molecule level. *Methods Enzymol* **475**: 259–278

- Tougu K, Marians KJ (1996) The interaction between helicase and primase sets the replication fork clock. *J Biol Chem* **271**: 21398–21405
- van Oijen AM, Loparo JJ (2010) Single-molecule studies of the replisome. *Annu Rev Biophys* **39**: 429–448
- Wu CA, Zechner EL, Reems JA, McHenry CS, Marians KJ (1992) Coordinated leading- and lagging-strand synthesis at the *Escherichia coli* DNA replication fork. V. Primase action regulates the cycle of Okazaki fragment synthesis. *J Biol Chem* **267**: 4074–4083
- Yao N, Turner J, Kelman Z, Stukenberg PT, Dean F, Shechter D, Pan ZQ, Hurwitz J, O'Donnell M (1996) Clamp loading, unloading and intrinsic stability of the PCNA,  $\beta$  and gp45 sliding clamps of human, *E. coli* and T4 replicases. *Genes Cells* **1**: 101–113
- Yao NY, Georgescu RE, Finkelstein J, O'Donnell ME (2009) Single-molecule analysis reveals that the lagging strand increases replisome processivity but slows replication fork progression. *Proc Natl Acad Sci USA* **106**: 13236–13241
- Yuzhakov A, Turner J, O'Donnell M (1996) Replisome assembly reveals the basis for asymmetric function in leading and lagging strand replication. *Cell* **86**: 877–886